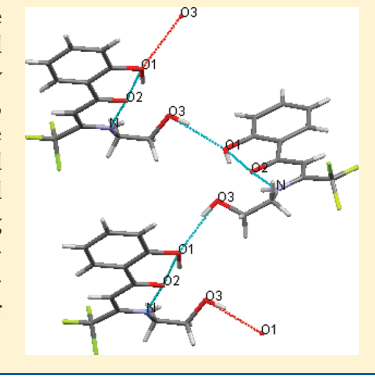
pubs.acs.org/JPCA

Spectroscopic, Structural, and Conformational Properties of (Z)-4,4, 4-Trifluoro-3-(2-hydroxyethylamino)-1-(2-hydroxyphenyl)-2-buten-1-one, $C_{12}H_{12}F_3NO_3$: A Trifluoromethyl-Substituted β -Aminoenone

A. Hidalgo, ^{†,‡} L. P. Avendaño Jiménez, [†] L. A. Ramos, [†] M. A. Mroginski, [§] J. L. Jios, ^{*,‡} S. E. Ulic, ^{*,†,⊥} G. A. Echeverría, [#] O. E. Piro, [#] and E. Castellano. $^{\nabla}$

Supporting Information

ABSTRACT: The (*Z*)-4,4,4-trifluoro-3-(2-hydroxyethylamino)-1-(2-hydroxyphenyl)-2-buten-1-one ($C_{12}H_{12}F_3NO_3$) compound was thoroughly studied by IR, Raman, UV—visible, and ¹³C and ¹⁹F NMR spectroscopies. The solid-state molecular structure was determined by X-ray diffraction methods. It crystallizes in the $P2_1/c$ space group with a=12.1420(4) Å, b=7.8210(3) Å, c=13.8970(5) Å, $\beta=116.162(2)^\circ$, and Z=4 molecules per unit cell. The molecule shows a nearly planar molecular skeleton, favored by intramolecular OH···O and NH···O bonds, which are arranged in the lattice as an OH···O bonded polymer coiled around crystallographic 2-fold screw-axes. The three postulated tautomers were evaluated using quantum chemical calculations. The lowest energy tautomer (I) calculated with density functional theory methods agrees with the observed crystal structure. The structural and conformational properties are discussed considering the effect of the intra- and intermolecular hydrogen bond interactions.



1. INTRODUCTION

The β -aminoenone N-C=C-C=O system is a structural moiety that constitutes an attractive and intricate subject to study. This conjugated moiety shows physical and chemical properties of both α,β -unsaturated carbonyl and enamine groups and for several decades has generated considerable interest as a useful multifunctional and relatively simple building block in synthetic and medicinal chemistry. $^{1-3}$ These compounds are another class of unsymmetrical pentad tautomeric systems, being the aminoenone, the iminoenol, and the iminoketone, the most stable tautomers (Scheme 1). In this prototropic tautomerism, the migration of three protons takes place; two of them are 1,3 shifts (keto-enol and imine-enamine), and the other one is a 1,5 proton shift (iminoenol-aminoenone).⁴ In more simple aminoenones such as β -aminoacrolein and its derivatives, the structure found in solid state is the nonchelated open chain form, but in solution a tautomeric equilibrium, which depends on the elected solvent, is established. These observations show that the

behavior of the aminoenones is more complicated and includes not only prototropie but also conformational and configurational equilibria. From the possible Z,E configurations and rotamers, only the planar structures allow a more effective stabilization by resonance. For β -aminoacrolein, 28 conformations are possible: 4 for the aminoenone, 16 for the iminoenol, and 8 for the ketoimine tautomeric forms. From them, the cyclic hydrogenbonded aminoenone form was found to be the most stable at the B3LYP/6-31G** level. On the contrary, in aromatic Schiff base compounds, the cyclic hydrogen-bonded iminoenol is the structure found in solid state and is also the predominant species in dissolution even in ethanol. Here, the resonance stabilization plays a determining role, shifting the equilibrium toward the imino form. UV spectroscopy was used successfully to study

Received: November 30, 2011
Revised: December 14, 2011
Published: January 13, 2012

[†]CEQUINOR (CONICET-UNLP), Facultad de Ciencias Exactas, Universidad Nacional de La Plata, 47 esq. 115, 1900 La Plata, República Argentina

[†]Departamento de Ciencias Básicas, Facultad de Ingeniería, Universidad Nacional de La Plata, 1 y 47, 1900 La Plata, República Argentina [§]Institut für Chemie, Max Volmer Laboratorium, Technische Universität Berlin, 10623 Berlin, Germany

LASEISIC-PLAPIMU (UNLP-CIC), Departamento de Química, Facultad de Ciencias Exactas, Universidad Nacional de La Plata,

República Argentina. 47 esq. 115, 1900 La Plata, Argentina

[⊥]Departamento de Ciencias Básicas, Universidad Nacional de Luján, Rutas 5 y 7, 6700 Luján, Buenos Aires, República Argentina [♯]Departamento de Física, Facultad de Ciencias Exactas, Universidad Nacional de La Plata e IFLP (CONICET, CCT-La Plata), C. C. 67, 1900 La Plata, Argentina

[▽]Instituto de Física de São Carlos, Universidade de São Paulo, C. P. 369, 13560 São Carlos (SP), Brazil

Scheme 1. Tautomeric Equilibria in the Title Compound

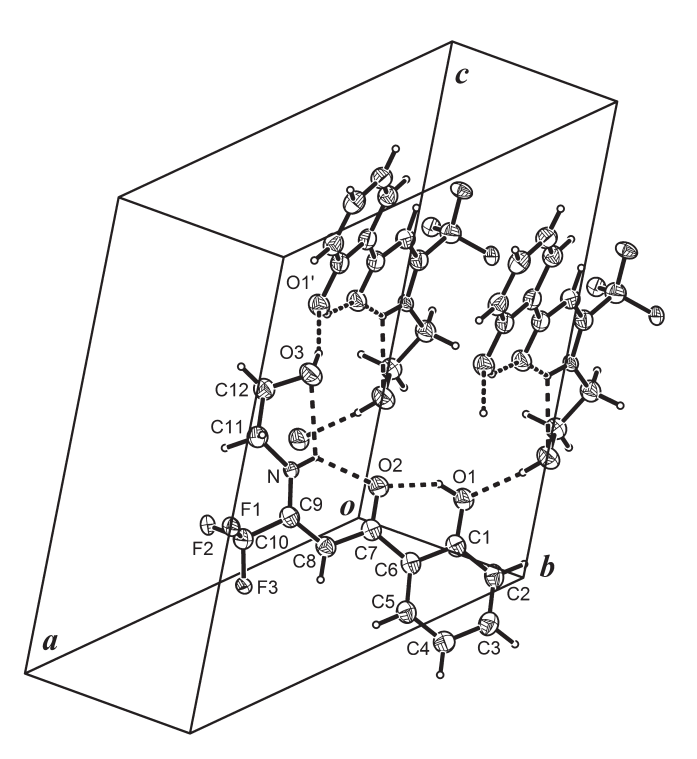


Figure 1. View of $C_{12}H_{12}F_3NO_3$ showing the labeling of the non-H atoms and their displacement ellipsoids at the 50% probability level. The intra- and intermolecular H-bonds are indicated by dashed lines.

both conformation and configuration equilibria in substituted $\beta\text{-aminoenones.}^{7-9}$ The position of the maximum absorption wavelength (λ) and the intensity (ε) of the $\pi \rightarrow \pi^*$ band is strongly influenced by both equilibria. On the basis of UV spectral data, the structure of the preferred conformation can be established. Moreover, the enamine moiety N-C=C- itself deserves particular attention since both N- and β -carbon atoms can operate as nucleophilic centers. The protonation site preference of the enamine was recently the subject of theoretical and experimental studies since their reactivity is directly related to their basicity. 10 Besides, the inclusion of a trifluoromethyl group in the $C\alpha$ geminal atom converts this aminoalkene in a captodative enamine expanding the electron delocalization possibilities to additional push-pull interactions. 10-12 The synthesis of β -aminoenones can be achieved by direct reaction with the appropriate amine (or ammonia) and a 1,3-diketone or 3-ketoester. In addition, β -trifluoromethylated β -aminoenones were obtained from trifluoropropynyl lithium and Weinreb amides. 13,14 In the past decade, the Sosnovskikh's group has synthesized several alkyl¹⁵ and aryl^{16–20} β -halomethylated β -aminoenones. The cleavage of 2-trifluoromethylchromones constitutes a simple method to obtain 2-hydroxyaroyl trifluoromethyl

enamines and was the selected strategy to prepare the title compound. ¹⁶ Other related aroyl enamines were also subjected to theoretical and experimental structural investigations. ²¹ In this case, the density functional theory (DFT) quantum-chemical calculations of the tautomers and conformers agree with structural X-ray and spectroscopic results. In this work we studied the title compound, considering the three main tautomeric forms (see Scheme 1), using single-crystal X-ray diffraction technique along with IR, Raman, and NMR spectroscopic methods, supported by quantum chemical calculations.

2. EXPERIMENTAL SECTION

2.1. Synthesis and Characterization of (*Z*)-4,4,4-Trifluoro-3-(2-hydroxyethylamino)-1-(2-hydroxyphenyl)-2-buten-1-one: $C_{12}H_{12}F_3NO_3$. The title compound was prepared according to literature ¹⁶ and recrystallized twice in hexane. The yellow crystalline solid (mp 104–105 °C) was suitable for the spectroscopic studies. Adequate single crystals for structural X-ray diffraction were obtained from slow evaporation at 20 °C of concentrated hexane solutions.

The ^1H NMR chemical shifts values agree very well with those reported 16 and are not described here. For the numbering of the phenyl carbon atoms see Figure 1. ^{13}C NMR (ppm): δ 194.1 (C=O), 162.4 (C-1), 150.5 (C-CF3, q, $^2J_{\text{C,F}}$ = 31 Hz), 135.3 (C-3), 128.4 (C-5), 120.3 (C-6), 120.1 (CF3, q, $^1J_{\text{C,F}}$ = 278 Hz), 119.0 (C-4), 118.7 (C-2), 88.6 (vinyl, q, $^3J_{\text{C,F}}$ = 3 Hz), 61.4 (CH2-O), and 46.8 (CH2-N). ^{19}F NMR (ppm): δ 66.9.

The UV—vis spectrum in methanol shows absorptions at $[\lambda \max{(nm)}]$ 365, 262, and 221.

The mass spectrum is shown in Figure S1 (Supporting Information): m/z (%) = 275 (M⁺, 18), 239 ([C₁₂H₈ONF₃]⁺, 12), 206 ([C₁₁H₁₂O₃N]⁺, 24), 140 ([C₄H₅ONF₃]⁺, 41), 121 ([HOPhC=O]⁺, 100), 93 ([C₆H₅O]⁺, 17), 86 ([C₄H₈ON]⁺, 31).

2.2. Instrumentation. *Infrared and Raman Spectroscopy.* Infrared spectra in KBr pellets were recorded on a LUMEX Infra LUM FT-02 spectrometer with a resolution of 2 cm⁻¹ in the range from 4000 to 400 cm⁻¹. Raman spectra of the solid (at room temperature) were measured in Pyrex standard capillaries (2.5 mm i.d.) on a Bruker IFS 66 spectrometer (spectral resolution, 4 cm⁻¹), equipped with a 1064 nm Nd:YAG laser, in the range from 4000 to 100 cm⁻¹.

NMR Spectra. The 1 H (200.0 MHz), 19 F (188.7 MHz), and 13 C (50.3 MHz) NMR spectra of the title compound were recorded at 298 K on a Varian Mercury Plus 200 spectrometer. The sample was dissolved in CDCl₃ in a 5 mm NMR tube. Chemical shifts, δ , for 13 C and 1 H NMR spectra are given in parts per million relative to tetramethylsilane (TMS; δ = 0 ppm) and are referenced by using the residual nondeuterated solvent signal. For 19 F NMR spectrum, a 0.05% trifluoroacetic acid (TFA) in CDCl₃ solution was used as external reference

Table 1. Crystal Data and Structure Refinement for (Z)-4,4,-4-Trifluoro-3-(2-hydroxyethylamino)-1-(2-hydroxyphenyl)-2-buten-1-one

empirical formula	$C_{12} H_{12} F_3 N O_3$
formula weight	275.23
temperature	100(2) K
wavelength	0.710 73 Å
crystal system	monoclinic
space group	$P2_1/c$
unit cell dimensions	a = 12.1420(4) Å
	b = 7.8210(3) Å
	c = 13.8970(5) Å
	$\beta = 116.162(2)^{\circ}$
volume	1184.49(7) Å ³
Z	4
density (calculated)	1.543 Mg/m^3
absorption coefficient	0.141 mm ⁻¹
F(000)	568
crystal size	$0.20 \times 0.18 \times 0.11 \text{ mm}^3$
crystal shape/color	prism/yellow
ϑ range for data collection	3.20-26.32°
index ranges	$-13 \le h \le 13, -9 \le k \le 8, -16 \le l \le 17$
reflections collected	13693
independent reflections	2210 [R(int) = 0.0643]
observed reflections	1968
completeness to θ = 26.32 $^{\circ}$	92.0%
max. and min transmission	0.9847 and 0.9724
refinement method	full-matrix least-squares on F^2
data/restraints/parameters	2210/0/175
goodness-of-fit on F ²	1.053
final <i>R</i> indices $[I > 2\sigma(I)]$	R1 = 0.0475, $wR2 = 0.1245$
R indices (all data)	R1 = 0.0524, $wR2 = 0.1293$
extinction coefficient	0.23(3)
largest diff. peak and hole	$0.199 \text{ and } -0.245 \text{ e.Å}^{-3}$

($\delta = -71.0$ ppm). Coupling constants, *J*, are reported in hertz, the quartet being marked as q.

 $UV-Visible\ Spectroscopy$. The spectra of $C_{12}H_{12}F_3NO_3$ in methanol were recorded using a quartz cell (10 mm optical path length) on a Chrom Tech CT-5700 UV/vis spectrophotometer, with 2.0 nm spectral bandwidth. Measurements were carried out in the spectral region from 190 to 700 nm.

Mass Spectrometry. A GC—MS Shimadzu QP-2010 was used to record the mass spectra. Details of the analysis conditions are given in Table S1 (Supporting Information).

X-ray Diffraction Data. Single-crystal X-ray diffraction measurements were performed at low temperature on an Enraf-Nonius Kappa-CCD diffractometer with graphite-monochromated Mo K α (λ = 0.710 73 Å) radiation. Diffraction data were collected (φ and ω scans with κ -offsets) with COLLECT. Integration and scaling of the reflections were performed with the HKL DENZO-SCALEPACK²³ suite of programs. The unit cell parameters were obtained by least-squares refinement based on the angular settings for all collected reflections using HKL SCALEPACK. Data were corrected numerically for absorption with PLATON. The structures were solved by direct and Fourier methods with SHELXS-97^{25,26} and the corresponding molecular models refined by full-matrix least-squares procedure

Table 2. Selected Calculated and Experimental Structural Parameters and Relative Energies of the Four Lowest Energy of $C_{12}H_{12}F_3NO_3$

			cal	$c^{b,d}$	
parameter ^a	$\operatorname{expt}^{b,c}(\operatorname{X-ray})$	I	II	III	IV
r(C7-C8)	1.432(2)	1.442	1.443	1.441	1.442
r(C6-C7)	1.481(2)	1.479	1.477	1.478	1.477
r(C8-C9)	1.373(2)	1.375	1.374	1.376	1.375
r(C9-C10)	1.517(2)	1.525	1.525	1.525	1.525
r(C11-C12)	1.503(2)	1.520	1.527	1.530	1.538
r(C7-O2)	1.265(2)	1.263	1.266	1.266	1.266
r(C9-N)	1.335(2)	1.345	1.348	1.346	1.346
r(C11-N)	1.464(2)	1.461	1.464	1.459	1.459
r(C12-O3)	1.423(2)	1.426	1.418	1.424	1.422
r(O3-H3A)	0.840(15)	0.961	0.964	0.962	0.963
r(O1-H1)	0.840(10)	0.991	0.989	0.989	0.989
\angle (C6-C7-C8)	120.45(13)	120.8	120.9	120.9	120.9
∠(C8-C9-C10)	117.89(13)	117.7	118.1	118.0	122.9
\angle (C8-C9-N)	125.97(14)	125.3	124.6	124.6	124.7
\angle (C9-N-C11)	128.21(13)	129.2	129.6	130.0	129.9
∠(C12-O3-H3A)	109.47(15)	109.7	108.8	109.2	109.2
∠(C1-O1-H1)	109.42(12)	106.5	106.7	106.6	106.7
φ(C5-C6-C7-C8)	0.00(24)	0.3	0.3	-0.6	-1.0
$\phi(C7-C8-C9-N)$	0.70(26)	1.4	-2.2	0.8	1.2
$\phi(N-C11-C12-O3)$	-60.61(17)	-61.0	-68.4	175.0	175.3
φ(C11-C12-O3-H3A)	160.07(14)	167.9	61.4	176.6	75.6
φ(C6-C1-O1-H1)	4.01(22)	0.1	-0.2	0.2	0.4
ΔE^{e} (kcal mol ⁻¹)		0.00	0.59	1.03	1.24

^a For labeling of the atoms see Figure 2. ^b Bond lengths in angstroms and angles in degrees. ^c Error limits given in parentheses are 3σ values for the last digit. ^d B3LYP/6-311++G(d,p) method was applied. ^e Calculated at the B3LYP/6-311++G(d,p) level of approximation.

on F^2 with SHELXL-97. The hydrogen atoms were included in the molecular model at stereochemical positions and refined with the riding method. The orientations of the OH groups were optimized by allowing them to rotate around the corresponding C-O bond. Crystal data and refinement results are summarized in Table 1. Crystallographic structural data have been deposited at the Cambridge Crystallographic Data Centre (CCDC). Enquiries for data can be directed to Cambridge Crystallographic Data Centre. Any request to the Cambridge Crystallographic Data Centre for this material should quote the full literature citation and the reference number CCDC 846797.

2.3. Quantum Chemical Calculation. Theoretical calculations were performed using the program package Gaussian 03. Scans of the potential energy surface, optimizations, and vibration frequency calculations of possible conformers of $C_{12}H_{12}F_3NO_3$ were carried out with the density functional theory (B3LYP) method employing the 6-311++G(d,p) basis set. The calculated vibrational properties correspond, in all cases, to potential energy minima with no imaginary values for the frequencies.

3. RESULTS AND DISCUSSION

3.1. Structural X-ray Diffraction. The crystal structure of the molecule is shown in Figure 1. The corresponding interatomic bond distances and angles are summarized in Table 2. The

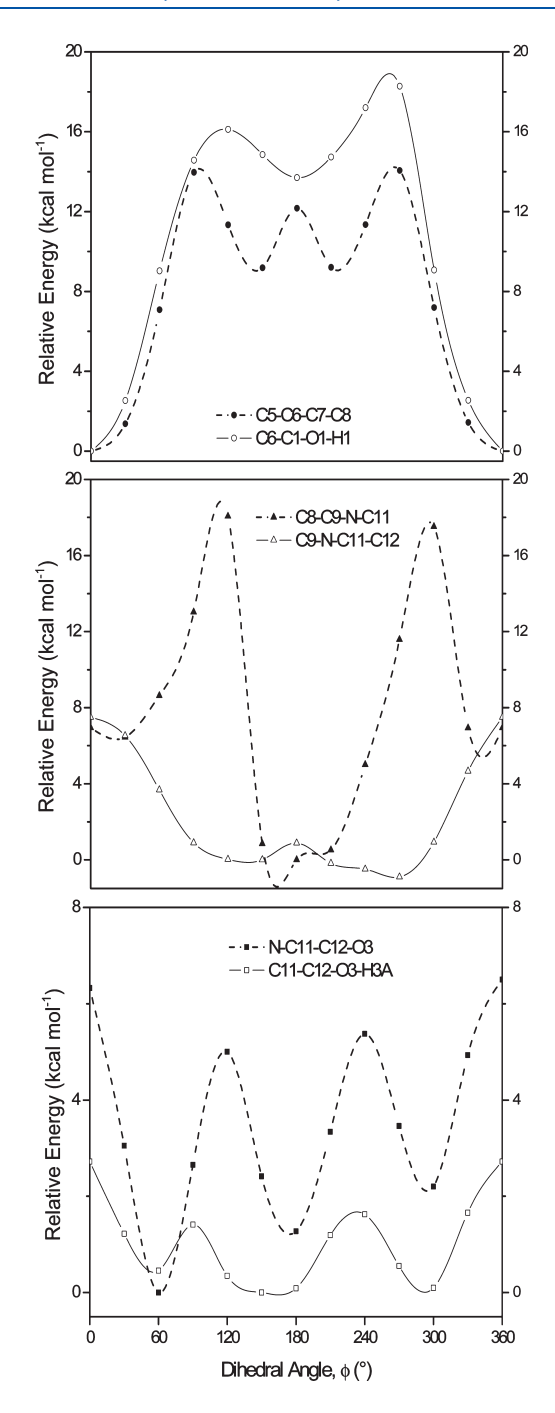


Figure 2. Potential energy curves for the internal rotation around the relevant bonds of $C_{12}H_{12}F_3NO_3$, calculated at the B3LYP/6-31G(d) level of theory.

representation of the crystal packing is shown in Figure S2 (Supporting Information). Observed bond distances agree with the organic chemistry rules. The phenol ring shows a delocalized bonding structure, with C–C distances in the range from 1.376(2) to 1.414(2) Å. We found the C(7)=O(2) and C(8)=C(9) distances of 1.265(2) and 1.373(2) Å, as expected for formally double bonds. The molecule conformation is stabilized by two strong intramolecular H-bonds, one involving a $O1-H\cdots O2$ interaction $[d(O1\cdots O2)=2.510(2)$ Å, $\angle -(O1-H\cdots O2)=147.1^{\circ}]$; the other one due to a $N-H\cdots O2$ bond $[d(N\cdots O2)=2.681(2)$ Å, $\angle (N-H\cdots O2)=129.6^{\circ}]$.

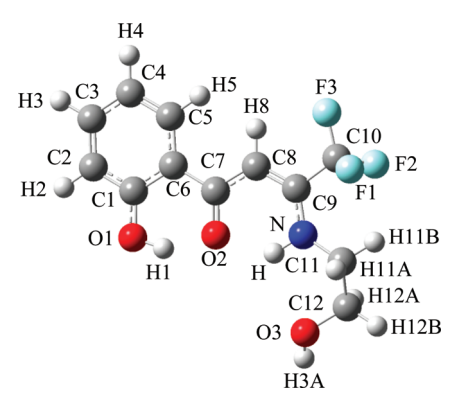


Figure 3. Optimized structure and labeling of the atoms for the lowest energy conformer (I) of $C_{12}H_{12}F_3NO_3$ at the B3LYP/6-311++G(d,p) level of theory.

Subjected to intramolecular steric hindrance and crystal packing interactions, these H-bonds tend to produce a nearly planar PhOH $-(C=O)-(CH)-C(CF_3)(NH)$ molecular skeleton (root mean square (rms) deviation of atoms from the least-squares plane of 0.083 Å) with the terminal $-(CH_2)_2OH$ group slightly departing from the plane but folded back to act as acceptor of a weak and bent intramolecular $N-H\cdots O3$ bond $[d(N\cdots O3)=2.787(2)$ Å, $\angle(N-H\cdots O3)=103.2^\circ]$. The crystal is further stabilized by intermolecular $O3-H\cdots O1'$ bonds involving the terminal hydroxyl of a molecule and the phenol oxygen of a 2-fold screw-axis symmetry-related neighboring molecule $[d(O3\cdots O1')=2.800(2)$ Å, $\angle(O3-H\cdots O1')=164.3^\circ]$. This gives rise to polymeric chains that extend along the crystal b-axis (see Figure 1).

3.2. Quantum Chemical Calculation. To evaluate the minimun energy structures adopted for the title compound, potential energy curves around several internal rotations were performed at the B3LYP/6-31G(d) level of theory (Figure 2). The structure is mainly characterized by a plane orientation of the C7-C8-C9-N central moiety. Besides, the rotation around the C6-C7 bond shows a local minimum energy with the phenolic ring coplanar with the C7-C8-C9-N skeleton; however, a second nonplanar orientation is expected at torsion angle $\phi(C5-C6-C7-C8) \approx 150^{\circ}$, but higher in energy by 9 kcal mol⁻¹ approximately. In addition, the lowest energy orientation of the OH group on the phenolic ring is in the *syn* position with respect to the C1–C6 bond $[\phi(C6-C1-O1-H1) \approx 0^{\circ}]$. Nevertheless, a second local minimum form is predicted in the anti orientation but quite higher in energy (\approx 14 kcal mol⁻¹) with respect to the syn form. This arrangement is only possible when the carbonyl group is distorted from planarity, which prevents the intramolecular hydrogen bond interaction.

On the other hand, the β -hydroxyethyl group is out of the C7–C8–C9–N plane at around 150°, as is shown in Figure 2. Moreover, two stable energy conformations are expected for the N–C11 with respect to the C12–O3 bond at 60 and 180°, with a relative energy difference (ΔE°) of 1.3 kcal mol⁻¹. Besides, the OH group could also adopt two stable orientations relative to the C11–C12 bond and with similar energies ($\Delta E^{\circ} \approx 0.5 \text{ kcal mol}^{-1}$).

Taking into account the high flexibility of this compound and that several possible conformations are expected to be above 6 kcal mol⁻¹ and consequently undetectable at room temperature, full optimizations of the four lowest energy conformers on the

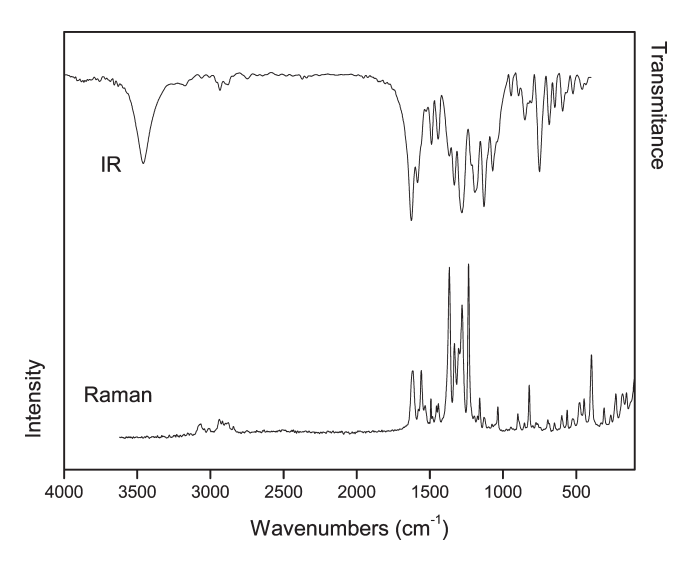


Figure 4. Infrared spectrum of the solid (upper trace, KBr pellets) and Raman spectrum of solid (lower trace) of $C_{12}H_{12}F_3NO_3$ at room temperature.

potential energy surface of the title compound were carried out by using the B3LYP/6-311++G(d,p) approximation. The calculated relative energies and geometrical parameters of these conformers are given in Table 2. Conformer I was predicted to be the most stable form (Figure 3). It exhibits a ϕ (N-C11-C12-O3) torsion angle of 61° and the OH group is anticlinal with respect to the C11-C12 bond (168°). The phenolic ring is in the same C7-C8-C9-C10 plane, while one fluorine atom of the CF₃ moiety eclipses the C8-C9 double bond. This arrangement guides the hydrogen atoms of the O1H1 and NH groups to the oxygen atom of the carbonyl group, which suggests the possibility of intramolecular hydrogen bonds $(O1-H1\cdots O2\cdots H-N)$. The short interatomic $O1\cdots O2$, O2···N, and N···O3 distance are 2.538, 2.668, and 2.805 Å, respectively, showing that these atoms are involved in intramolecular hydrogen interactions. Such interactions are relevant to stabilize the predicted conformation. Moreover, the resonance assisted hydrogen bond (RAHB) model³³ allows one to explain the electronic charge delocalization along the C7-C8 and C9-N bonds in the O=C-C=C-N-H system. The optimized structure shows for them certain double bond character, as observed in Figure 3 (dashed lines).

In addition, values of 2.510, 2.681, and 2.787 Å are obtained from X-ray diffraction analysis for the analogous intramolecular hydrogen bonding. This good agreement between theoretical calculations and X-ray diffraction results stresses the relevance of these interactions in both solid and gas phases.

On the other hand, the second stable form (II) is higher in energy than I by 0.59 kcal mol⁻¹, and the main difference is for $\phi(C11-C12-O3-H3A)=61^{\circ}$. The III and IV conformers differ from the I and II ones mainly by the dihedral angles $\phi(N-C11-C12-O3)$ with values of 175° approximately, and the optimized values of $\phi(C11-C12-O3-H3A)$ of the forms III and IV result not very different from those in I and II. The calculated energy differences of III and IV rotamers with respect to the most stable conformer (I) are relatively low and resulted in 1.03 and 1.24 kcal mol⁻¹, respectively. With these energy difference values, rotational equilibria at room temperature are possible; however, only one conformer is observed in the X-ray

crystal structure (see crystal structure section) with an atomic arrangement similar to the predicted for the most stable conformer (I). The experimental and calculated differences are in principle reasonable considering that the calculations are performed for the molecule in the gas phase, where the intermolecular interactions produced in the crystal lattice are not taken into account.

3.3. Vibrational Spectra. Only the most relevant characteristic functional groups of the molecule will be analyzed. The IR and Raman spectra of the solid compound are shown in Figure 4 and the tentative assignment of the observed and computed fundamental vibrational modes are presented in Table 3.

The weak O-H stretching band, corresponding to the nonchelated hydroxylic group, predicted at 3855 cm⁻¹ is not observed in the IR and Raman spectra. On the other hand, the in-plane deformation band is observed at 1219 cm⁻¹ in IR (calculated value, 1220 cm⁻¹) and is undetected in Raman, whereas that out-of-plane bending predicted at 256 cm⁻¹ was detected at 264 cm⁻¹ in Raman. The low estimated IR frequency could indicate the absence of hydrogen bonding through this hydroxyl group, ^{34,35} otherwise the force constant increases, resulting in a shift toward higher wavenumbers.

The medium intense band observed at 3459 cm⁻¹ (calculated, 3278 cm⁻¹) is attributed to the Ph-OH group. Moreover, the free O-H stretching vibration of phenols gives rise to a sharp band between 3700 and 3600 cm⁻¹ in the gas phase. The presence of ortho substituents, in particular of a hydrogen bond acceptor group in this position, leads to intramolecular hydrogen bonding effects. Participation of the O-H proton in hydrogen bonding leads to a marked red shift of the O-H stretching band and usually along with the broadening of the band. The formation of an intramolecular hydrogen bond often results in the closing of a five- or six-membered pseudoring structure 34,36,37 and even more, stronger intramolecular hydrogen bonding is expected for phenols with NO2, R-C=O, or R-C=N-R groups in the 2-position.³⁶ This interaction is frequently denominated as "chelation". The stronger the chelated hydrogen bond, the lower the recorded IR intensity, which results opposite to that observed for intermolecular hydrogen bonding, frequently associated with an increase in the integrated IR intensity.

The in-plane bending mode is assigned to the Raman band at 1441 cm⁻¹, while the out-of-plane bending, to the band at 852 cm⁻¹ in IR (calculated, 842 cm⁻¹). It is also evident, by the position of this band (blue-shifted), the participation of the O–H group in hydrogen bonding interactions.

The weak bands in the Raman spectra at 3072, 3043, 3010, and 2939 $\rm cm^{-1}$ are assigned to the C–H stretching modes of the ring 38 (see Table 3) and those at 2917, 2897, 2881, and 2843 $\rm cm^{-1}$ to the stretching modes of the CH $_2$ group. The intensities and the band positions are in good agreement with the predicted values by quantum chemical calculations.

The $\nu(N-H)$ band could not be observed in IR and Raman possibly because of its low intensity and by overlapping with the broad band of the O-H group attached to the ring. The in-plane deformation of the N-H group can be attributed to the band at 1364 cm⁻¹ (IR) and 1367 cm⁻¹ (Raman), whereas that the calculated value for this mode resulted in 1364 cm⁻¹. The out-of-plane bending mode expected at 823 cm⁻¹ is assigned to the IR band at 802 cm⁻¹ and to the band at 796 cm⁻¹ in Raman. The observed wavenumbers are in agreement with reported values of related amines. ^{39,40}

 $\label{eq:continuous_continuous$

		exptl		lcd ^b	
mode	IR ^a	Raman	frequency	intensity	assignment $^{[c]}$
' 1			3855	53	ν(O3-H3)
' 2			3395	66	$ u({ m N-H}) $
' ₃	3459 m		3278	431	u(01-H1)
' ₄	3172 vw		3276	78	$\nu(\text{C8-H8})$
v ₅	3063 vw	3072(8)	3205	9	ν (C2–H2) + ν (C3–H3) + ν (C4–H4) + ν (C5–H5) (in phase)
' ₆		3043(6)	3196	11	ν (C2-H2) + ν (C3-H3) + ν (C5-H5)
v ₇	3006 vw	3010(6)	3186	10	ν (C2–H2) + ν (C3–H3) + ν (C4–H4) + ν (C5–H5) (out of phase)
ν_8	2936 w	2939	3169	5	ν (C2-H2) + ν (C3-H3) + ν (C4-H4)
V ₉		2917	3129	11	$v_{\rm as}({\rm C}11{\rm -H_2})$
' ₁₀	2899 vw	2897	3043	78	$v_{\rm as}({\rm C}12{ m -H_2})$
' ₁₁	2878 w	2881	3019	10	$v_{\rm s}({\rm C}11-{\rm H}_2)$
' ₁₂	2838 vw	2843	2998	63	$v_{\rm s}({\rm C}12{\rm -H_2})$
' ₁₃			1662	54	$\nu(\text{C1-C2}) + \nu(\text{C4-C5}) + \nu(\text{C8-C9}) + \delta(\text{H-N-C9})$
' ₁₄	1626vs	1617(39)	1659	916	ν (C7-02) + ν (C8-C9) + δ (H-N-C9)
' ₁₅	1583 m	1578(17)	1614	242	$v(C2-C3) + \delta(H-O1-C1)$
' ₁₆		` /	1593	64	$\delta(H-O1-C1) + \delta(H-N-C9) + \nu(C7-02)$
' ₁₇	1560 w	1558(39)	1552	50	ν (C9- N) + ν (C7-C8) + δ (C7-C8-H)
' ₁₈		1533(19)	1520	79	$\delta(\text{C2-H2}) + \delta(\text{C3-H3}) + \delta(\text{C4-H4}) + \delta(\text{C5-H5})$
' ₁₉			1512	7	δ (C12-H ₂)
20	1490 w	1493(23)	1492	35	δ (C11-H ₂)
'21	1456 w	1455(17)	1473	56	$\delta(\text{C2-H}) + \delta(\text{C3-H}) + \delta(\text{C4-C5}) + \nu(\text{C1-01})$
'22		,	1448	5	$\delta_{\text{wag}}(\text{C12-H}_2)$
'23	1441 m	1441(20)	1434	36	δ (01–H1) + δ _{wag} (C11–H ₂)
y ₂₄		(21)	1419	92	$\nu(\text{C4-C5}) + \nu(\text{C8-C9}) + \delta(\text{C5-C6-C7})$
'25	1364 m	1367(83)	1364	372	$\delta(H-N-C9) + \nu(C9-C10) + \nu(C6-C7)$
² 26		-517 (15)	1355	16	$\delta(H-N-C9) + \nu(C8-C9) + \nu(C7-C8)$
v ₂₇	1335 m	1333(54)	1336	123	$\delta_{\text{twi}}(\text{C11-H}_2) + \nu(\text{C1-O1})$
, 28	1299 s	1304(52)	1321	141	$\delta_{\text{twi}}(\text{C11-H}_2) + \delta_{\text{twi}}(\text{C12-H}_2)$
'29	1283 vs	1280(77)	1298	277	$\delta(H-C8-C7) + \nu(C9-C10)$
y ₃₀	1237 m	1236(100)	1274	239	$\delta_{\text{twi}}(\text{C12-H}_2) + \nu(\text{C5-C6})$
'31		()	1268	14	$\delta_{\text{twi}}(\text{C12-H}_2)$
'32			1237	83	ν(C6–C7)
'33	1219 s		1220	75	$\delta(\text{H3-O3}) + \delta(\text{H-C11-N})$
'33 '34	1196 vs	1197(12)	1201	107	$v_s(CF_3) + v(N-C11) + v(C9-C10)$
³⁴ ³⁵	1178 vs	1174(13) 1160(23)	1185	177	$\delta(\text{C2-H}) + \delta(\text{C3-H}) + \delta(\text{C4-H}) + \delta(\text{C5-H})$
y ₃₆	1130 vs	1130(12)	1166	219	$v_{\rm as}(\text{C-F}_3) + \delta(\text{C2-H}) + \delta(\text{C3-H})$
y ₃₇		\	1148	26	$\delta(\text{C2-H}) + \delta(\text{C3-H})$
y ₃₈			1123	75	δ (C8-C9-N)
y ₃₉	1076 s	1076(8)	1105	265	$v_{\rm as}({ m CF}_3)$
y ₄₀		ν-/	1085	37	ν(C12-O3)
y ₄₁			1067	85	ν(C11-C12)
41	1048 w		1060	4	$\nu(\text{C3-C4}) + \delta(\text{C2-H}) + \delta(\text{C5-H})$
42 '43	1033 m	1036(18)	1053	41	$\nu(\text{C3-C4}) + \nu(\text{C7-C8})$
43 7 ₄₄			986	<1	$\gamma(\text{C2-H}) + \gamma(\text{C3-H}) + \gamma(\text{C4-H})$
, 44 , 45	948 m		954	8	$\nu(\text{C11-C12})$
) .O III		948	1	$\gamma(\text{C4-H}) + \gamma(\text{C5-H})$
y 46	899 w	899(14)	909	22	$\delta(O2 - C7 - C8) + \delta_{wag}(C11 - H2)$
47 40	5// W	U//(17)	867	<1	$\gamma(\text{C2-H}) + \gamma(\text{C3-H}) + \gamma(\text{C4-H}) + \gamma(\text{C5-H}) + \gamma(\text{O1-H})$
⁷ 48			865	6	$\delta(C3-C4-C5)$
ν_{49}	852 m	853(9)	842	U	$\gamma(O1-H1) + \gamma(N-H)$

Table 3. Continued

	exptl		$calcd^b$		
mode	IR ^a	Raman	frequency	intensity	assignment $^{[c]}$
ν_{51}	822 w	822(30)	835	5	δ (C3-C4-C5) + δ (C7-C8-C9) + ν (N-C11)
v_{52}	802 w	796(7)	823	18	$\gamma({ m N-H})$
ν_{53}			802	5	γ (C8-H8)
ν_{54}		774(9)	773	6	$\delta_{ m s}({ m CF}_3)$
ν_{55}	754 s		767	112	γ (C2-H2) + γ (C3-H3) + γ (C4-H4) + γ (C5-H5) + γ (C8-H8)
v_{56}			743	<1	γ (C8–H8) + γ (C2–H2) + γ (C3–H3) + γ (C4–H4) + γ (C5–H5)
ν_{57}			701	2	γ (C8-H8) + γ (C2-H2) + γ (C4-H4) + γ (N-H)
ν_{58}	691 w	694(11)	698	12	$\delta(\text{C1-C6-C5}) + \delta(\text{C1-C2-C3}) + \delta(\text{C2-C3-C4}) + \delta(\text{C8-C9-N})$
ν_{59}	682 w	684	683	4	γ (C8-C9-N)
ν_{60}	648 w	648(9)	656	45	$\delta(C6-C7-O2) + \delta(C8-C9-C10)$
ν_{61}	598 w	598(13)	596	30	$\delta(N-C11-C12) + \delta_s(CF_3)$
ν_{62}	562 vw	562(16)	569	3	$\delta(C3-C4-C5) + \delta(C1-C2-C3)$
ν_{63}			530	5	γ (C2-H2) + γ (C3-H3) + γ (C5-H5)
ν_{64}	526 vw	523(11)	520	4	$\delta_{as}(CF_3) + \delta(N-C11-C12) + \delta(C6-C7-C8)$
ν_{65}			514	1	$\delta_{ m as}({ m CF}_3)$
v_{66}			483	1	$\delta(O1-C1-C6) + \delta(C11-C12-O3)$
ν_{67}		478(20)	466	8	δ (C9-N-C11) + (C11-C12-O3) + δ _{as} (CF3)
ν_{68}		446(21)	449	8	$\delta(C6-C7-C8) + \delta(C11-C12-O3)$
ν_{69}			439	2	$\gamma(C5-C6-C7) + \gamma(C1-C2-C3)$
ν_{70}		396(48)	393	4	δ (C1–C6–C7)
ν_{71}		330(9)	343	11	δ (C9-N-C11) + τ (N-C11-C12-O3)
ν_{72}		310(17)	307	1	τ (N-C11-C12-O3)
ν_{73}			305	2	τ (C9-N-C11-C12) + γ (C7-C8-C9)
ν_{74}		264(13)	256	98	γ(O3-H3)
ν_{75}			249	25	γ (O3-H3) + γ (C1-O1)
ν_{76}		229(26)	225	2	δ (C7–C8–C9)
ν_{77}		184(25)	224	15	$\delta(C8-C9-N) + \tau(N-C11-C12-O3)$
ν_{78}			167	1	γ (H–N–C11)
ν_{79}		157(26)	155	2	τ (N-C11-C12-O3) + τ (C1-C6-C7-C8)
ν_{80}			140	1	τ (O2-C7-C8-C9)
ν_{81}			113	1	$\delta(N-C11-C12) + \delta(C6-C7-C8)$
ν_{82}			103	2	τ (C9-N-C11-C12) + τ (C11-C12-O3-H)
ν_{83}			77	2	τ(C10-C9-N-C11)
ν_{84}			64	1	δ (C9-N-C11) + δ (C6-C7-C8)
ν_{85}			32	1	τ (C9-N-C11-C12)
ν_{86}			30	1	τ (C10-C9-N-C11) + γ (C6-C7-C8)
ν_{87}			21	2	τ (C5-C6-C7-C8) + τ (C9-N-C11-C12)

^a vs, very strong; s, strong; w, weak; vw, very week; sh, shoulder. ^b B3LYP/6-311+G(d) and calculated IR intensities in kilometers per mole. ^[c] ν , δ , γ , and τ represent stretching, in plane deformation, out-of-plane deformation, and torsion modes.

The $\nu(C=O)$ vibrational mode is associated with the very strong IR band at $1626~{\rm cm}^{-1}$ and with the weak absorption at $1617~{\rm cm}^{-1}$ in Raman, while the calculated value results in $1659~{\rm cm}^{-1}$. The observed wavenumber for this mode indicates that this group is involved in intra- and intermolecular interactions. Besides, this mode is strongly coupled with the aliphatic $\nu(C=C)$, which is predicted at $1662~{\rm cm}^{-1}$. This mode is observed at $1660~{\rm and}~1647~{\rm cm}^{-1}$ in methoxy and methyl substituted acetophenones.

The CF₃ vibrational modes observed at 1196, 1130, and $1076~{\rm cm}^{-1}$ in IR, and at 1197, 1130, and $1076~{\rm cm}^{-1}$ in Raman are assigned to $\nu_{\rm s}{\rm CF}_3$, $\nu_{\rm as}{\rm CF}_3$, and $\nu_{\rm as}{\rm CF}_3$, respectively (calculated, 1201, 1166, and 1105 cm⁻¹). In addition, the bands

at 774, 598, and 523 cm⁻¹ in the Raman spectra (IR: only two bands observed at 598 and 526 cm⁻¹; calc. 773, 596, and 520 cm⁻¹) are attributed to the δ_s CF₃, δ_{as} CF₃, and δ_{as} CF₃, respectively.

3.4. NMR Spectra. The observed NMR spectra are consistent with tautomeric equilibria in CDCl₃ dissolution shifted to the aminoenone form (see Scheme 1). The o-hydroxyphenylcarbonyl moiety shows a proton strongly coupled to the oxygen of the carbonyl group at 12.65 ppm. ¹⁶ This value is even higher than that found in the tautomeric 1-(o-hydroxyphenyl)-3-aryl-1, 3-propanediones (δ 12.11–12.13 ppm). ⁴² Consequently the N–H proton appears at 11.55 indicating hydrogen bond interaction but of lower intensity compared with the enol O–H (δ 15.60–15.61 ppm). ⁴² Considering that the capacity of the

carbonyl oxygen as a base remains constant, the weakening of the $N-H\cdots O$ interaction should reinforce the phenolic $O-H\cdots O$ hydrogen bond in the title compound. Besides, no detectable signals of the iminoketo form could be found. Such tautomer should show the methylene signals at ca. 4.7 and 52 ppm, for 1H and ^{13}C spectra, respectively.

4. CONCLUSION

According to the results of quantum chemical calculations, the title compound adopts, as the most stable the conformation I, that keeps both the ring and the C7–C8–C9–N skeleton in a plane and the hydroxyethyl pendant out of this plane with two consecutive torsion angles $\phi(N-C11-C12-O3)$ and $\phi(C11-C12-O3-H)$ of 61 and 168°, respectively. Besides, X-ray crystal structure determination shows also an atomic arrangement similar to the predicted form I. The intramolecular hydrogen bond interactions seem to play an important role in stabilizing the calculated geometry in the gas phase. Such interactions are also of important in the solid phase, considering the good agreement between theoretical calculations and X-ray diffraction results in the O1···O2, N···O2, and N···O3 interatomic distances.

The location, intensity, and the shape of the phenolic O—H vibrational modes, observed in the IR spectra, confirm the prevalence of intramolecular hydrogen bonding interactions, in concordance with reported data for related compounds.

ASSOCIATED CONTENT

Supporting Information. Mass spectrum of $C_{12}H_{12}F_3NO_3$ (Figure S1), view of the unit cell along the *b*-axis (Figure S2), GC-MS conditions used in the analysis of $C_{12}H_{12}F_3NO_3$ (Table S1), atomic coordinates and equivalent isotropic displacement parameters (Table S2), full structural parameters (Table S3), anisotropic displacement parameters (Table S4), and hydrogen coordinates and isotropic displacement parameters (Table S5). This material is available free of charge via the Internet at http://pubs.acs.org.

AUTHOR INFORMATION

Corresponding Author

*E-mail: jljios@quimica.unlp.edu.ar (J.L.J.); sonia@quimica.unlp.edu.ar (S.E.U.).

■ ACKNOWLEDGMENT

We thank Universidad Nacional de La Plata (UNLP), CONICET, DAAD-Germany, and Departamento de Ciencias Básicas de la Universidad Nacional de Luján for financial support. S.E.U. and J.L.J. especially thank Deutscher Akademischer Austauschdienst Germany (DAAD) for the equipment grant and financial support. A.H. thanks Facultad de Ingeniería de la Universidad Nacional de La Plata for the fellowship. Part of this work was also supported by CONICET (Grant PIP 1529) and by ANPCyT (Grants PME06 2804 and PICT06 2315) of Argentina and FAPESP of Brazil. S.E.U., G.A.E., and O.E.P. are research fellows of CONICET.

■ DEDICATION

Dedicated to Professor Helge Willner, on the occasion of his 65th birthday.

■ REFERENCES

- (1) Greenhill, J. V. Chem. Soc. Rev. 1977, 6, 277.
- (2) Gorobets, N. Y.; Sedash, Y. V.; Shishkina, S. V.; Shishkin, O. V.; Yermolayev, S. A.; Desenko, S. M. *ARKIVOC (Gainesville, FL, U. S.)* **2009**, 23 (Part xiii).
- (3) Alberola, A.; Calvo, L. A.; Ortega, A. G.; Ruíz, M. C. S.; Yustos, P. J. Org. Chem. 1999, 64, 9493.
- (4) Raczyńska, E. D.; Kosińska, W.; Ośmiałowski, B.; Gawinecki, R. Chem. Rev. 2005, 105, 3561.
- (5) Buemi, G.; Zuccarello, F.; Venuvanalingam, P.; Ramalingam, M. *Theor. Chem. Acc.* **2000**, *104*, 226.
 - (6) Tanak, H. J. Phys. Chem. A 2011, 115, 13865.
 - (7) Ostercamp, D. L. J. Org. Chem. 1970, 35, 1632.
- (8) Dabrowski, J.; Kamieńska-Trela, K. J. Am. Chem. Soc. 1976, 98, 2826.
- (9) Kania, L.; Kamieńska-Trela, K.; Witanowski, M. J. Mol. Struct. 1983, 102, 1.
 - (10) Rulev, A. Y.; Ushakov, I. A. J. Fluorine Chem. 2010, 131, 53.
 - (11) Rulev, A. Y.; Zinchenko, S. V. Mendeleev Commun. 2001, 11, 70.
- (12) Chipanina, N. N.; Aksamentova, T. N.; Shainyan, B. A.; Rulev, A. Y. J. Mol. Struct. (THEOCHEM) **2010**, 947, 22.
- (13) Jeong, I. H.; Jeon, S. L.; Kim, M. S.; Kim, B. T. J. Fluorine Chem. **2004**, 125, 1629.
- (14) Jeong, I. H.; Jeon, S. L.; Min, Y. K.; Kim, B. T. Tetrahedron Lett. **2002**, 43, 7171.
- (15) Sosnovskikh, V. Y.; Mel'nikov, M. Y. Mendeleev Commun. 1998, 8, 243.
- (16) Sosnovskikh, V. Y.; Usachev, B. I. Mendeleev Commun. 2000, 10, 240.
- (17) Sosnovskikh, V. Y.; Kutsenko, V. A.; Yachevskii, D. S. Mendeleev Commun. 1999, 9, 204.
- (18) Sosnovskikh, V. Y.; Kutsenko, V. A.; Morozov, M. Y. Mendeleev Commun. 1998, 8, 126.
 (19) Sosnovskikh, V. Y.; Usachev, B. I. Mendeleev Commun. 2002,
- 12, 75.
- (20) Sosnovskikh, V. Y.; Kutsenko, V. A. Mendeleev Commun. 1999, 9, 206.
- (21) Jezierska, A.; Jerzykiewicz, L. B.; Kolodziejczak, J.; Sobczak, J. M. J. Mol. Struct. 2007, 839, 33.
- (22) Enraf-Nonius. COLLECT; Nonius BV: Delft, The Netherlands, 1997-2000.
- (23) Otwinowski, Z.; Minor, W. In *Methods in Enzymology*; Carter, C. W., Jr., Sweet, R. M., Eds.; Academic Press: New York, 1997; Vol. 276; p 307.
- (24) Spek, A. L. PLATON, A Multipurpose Crystallographic Tool; Utrecht University: Utrecht, The Netherlands, 1998.
- (25) Sheldrick, G. M. SHELXS-97. Program for Crystal Structure Resolution; University of Göttingen: Göttingen, Germany, 1997.
 - (26) Sheldrick, G. Acta Crystallogr., Sect. A 1990, 46, 467.
 - (27) Sheldrick, G. Acta Crystallogr., Sect. A 2008, 64, 112.
- (28) Frisch, M. J.; Trucks, G. W.; Schlegel, H. B.; Scuseria, G. E.; Robb, M. A.; Cheeseman, J. R.; Montgomery J. A., Jr.; Vreven, T.; Kudin, K. N.; Burant, J. C.; Millam, J. M.; Iyengar, S. S.; Tomasi, J.; Barone, V.; Mennucci, B.; Cossi, M.; Scalmani, G.; Rega, N.; Petersson, G. A.; Nakatsuji, H.; Hada, M.; Ehara, M.; Toyota, K.; Fukuda, R.; Hasegawa, J.; Ishida, M.; Nakajima, T.; Honda, Y.; Kitao, O.; Nakai, H.; Klene, M.; Li, X.; Knox, J. E.; Hratchian, H. P.; Cross, J. B.; Adamo, C.; Jaramillo, J.; Gomperts, R.; Stratmann, R. E.; Yazyev, O.; Austin, A. J.; Cammi, R.; Pomelli, C.; Ochterski, J. W.; Ayala, P. Y.; Morokuma, K.; Voth, G. A.; Salvador, P.; Dannenberg, J. J.; Zakrzewski, V. G.; Dapprich, S.; Daniels, A. D.; Strain, M. C.; Farkas, O.; Malick, D. K.; Rabuck, A. D.; Raghavachari, K.; Foresman, J. B.; Ortiz, J. V.; Cui, Q.; Baboul, A. G.; Clifford, S.; Cioslowski, J.; Stefanov, B. B.; Liu, G.; Liashenko, A.; Piskorz, P.; Komaromi, I.; Martin, R. L.; Fox, D. J.; Keith, T.; Al-Laham, M. A.; Peng, C. Y.; Nanayakkara, A.; Challacombe, M.; Gill, P. M. W.; Johnson, B.; Chen, W.; Wong, M. W.; Gonzalez, C.; Pople, J. A. Gaussian 03, Revision B.04 ed.; Gaussian: Pittsburgh, PA, USA, 2003.

- (29) Becke, A. D. Density-Functional Thermochemistry. III. The Role of Exact Exchange; American Institute of Physics: New York, 1993; Vol. 98.
 - (30) Lee, C.; Yang, W.; Parr, R. G. Phys. Rev. B 1988, 37, 785.
- (31) Perdew, J. P.; Burke, K.; Ernzerhof, M. Phys. Rev. Lett. 1996, 77, 3865.
- (32) Perdew, J. P.; Burke, K.; Ernzerhof, M. Phys. Rev. Lett. 1997, 78, 1396.
- (33) Gilli, P.; Bertolasi, V.; Ferretti, V.; Gilli, G. J. Am. Chem. Soc. **2000**, 122, 10405.
- (34) Hansen, P. E.; Spanget-Larsen, J. NMR and IR Spectroscopy of Phenols. In *The Chemistry of Phenols*; Rappoport, Z. Z., Ed.; Wiley: Chichester, U.K., 2003.
- (35) Keresztury, G.; Billes, F.; Kubinyi, M.; Sundius, T. J. Phys. Chem. A 1998, 102, 1371.
- (36) Hibbert, F.; Emsley, J.; Bethell, D. Hydrogen Bonding and Chemical Reactivity. In *Advances in Physical Organic Chemistry*; Academic Press: New York, 1991; Vol. 26, p 255.
- (37) Rostkowska, H.; Nowak, M. J.; Lapinski, L.; Adamowicz, L. Phys. Chem. Chem. Phys. 2001, 3, 3012.
- (38) Michalska, D.; Bieńko, D. C.; Abkowicz-Bieńko, A. J.; Latajka, Z. J. Phys. Chem. **1996**, 100, 17786.
- (39) Korolevich, M. V.; Sivchik, V. V.; Matveeva, N. A.; Zhbankov, R. G.; Lastochkina, V. A.; Frenkel, M. L.; Ladut'ko, A. I.; Pavlov, A. V.; Petryaev, E. P. *J. Appl. Spectrosc.* **1987**, *46*, 400.
 - (40) Verma, A. L. Spectrochim. Acta, Part A 1971, 27, 2433.
- (41) Krishnakumar, V.; Balachandran, V. Spectrochim. Acta, Part A 2005, 61, 2510.
 - (42) Jios, J. L.; Duddeck, H. Z. Naturforsch. 2000, 55b, 193.